

Valproic acid substantially downregulated genes *folr1*, *IGF2R*, *RGS2*, *COL6A3*, *EDNRB*, *KLF6*, and *pax-3*, N-acetylcysteine alleviated most of the induced gene alterations in chicken embryo model

CHIU-LAN HSIEH^{1)†}, KUAN-CHOU CHEN^{2,3)†}, CHI-YANG DING¹⁾,
 WAN-JANE TSAI¹⁾, JIA-FONG WU¹⁾, CHIUNG-CHI PENG⁴⁾

¹⁾Graduate Institute of Biotechnology,
 Changhua University of Education, Changhua, Taiwan

²⁾Department of Urology,
 School of Medicine, College of Medicine,
 Taipei Medical University, Taipei, Taiwan

³⁾Department of Urology,
 Shuang Ho Hospital,
 Taipei Medical University, Zhonghe, Taipei, Taiwan

⁴⁾Graduate Institute of Clinical Medicine,
 College of Medicine,
 Taipei Medical University, Taipei, Taiwan

[†]The two authors contributed equally to the manuscript.

Abstract

Valproic acid induced teratogenicity at genetic and somatic levels, the action mechanism is still unclear. We hypothesized that folate receptor gene (*folr1*) and others may be interacting to elicit neural tube defect (NTD), while N-acetylcysteine (NAC) may be beneficial for protection. In chicken embryo model, the experiment was conducted in two parts. The first part was carried out to test the optimum dose of VPA. The second part was conducted to test the protective effect of NAC at doses 10 and 20 mM. VPA induced dysvascularization, incomplete somite enclosure, histone deacetylase (HDAC) inhibition, folate deficiency, homocysteine accumulation, SOD inhibition, glutathione depletion, elevated MDA and hydrogen peroxide. NAC alleviated most of these adverse effects. The microarray analysis revealed 17 genes downregulated and four upregulated. The relevancy covered translation (23%), signal transduction (23%), transcription (16%), cell adhesion (16%), neural cell migration (8%), transport (7%), and organismal development (7%). The genes insulin-like growth factor 2 receptor gene (*IGF2R*), regulator of G-protein signaling 4 gene (*RGS4*), alpha 3 (VI) collagen gene (*COL6A3*), endothelin receptor type b gene (*EDNRB*), and Krüppel-like factor 6 gene (*KLF6*) substantially downregulated in reality were directly intermodulating and associated with NTD. VPA downregulated *folr1* gene in a dose responsive manner without affecting *pax-3* gene, which was ascribed to the metahypoxic state. Conclusively, VPA affects 21 genes: 17 downregulated and four upregulated. VPA dose responsively downregulates gene *folr1* without affecting *pax-3* gene. These adverse effects can be partially alleviated by N-acetylcysteine.

Keywords: valproic acid teratogenicity, N-acetylcysteine, folate receptor gene *folr1*, *pax-3* gene, neural tube defect (NTD), histone deacetylase inhibitor.

Introduction

The teratogenic potential of valproic acid (VPA) has been well established in both experimental models and human clinical studies [1]. Before organogenesis, the avascular embryo is physiologically hypoxic (2–5% O₂). Dysvascularization with increased glucose metabolic rate in developing embryos could exacerbate the hypoxic state [1, 2]. Excessive hypoxia in turn may contribute to oxidative stress [2]. VPA elicits teratogenicity by (i) promoting folic acid deficiency [1] and acting as a disrupter of methylene tetrahydrofolate reductase (MTHFR) [3]; (ii) inducing oxidative stress [4]; (iii) leading to the ω - and β -oxidation [5]; (iv) inhibiting

histone deacetylase (HDAC) [1]; (v) counteracting angiogenesis [6]; and (vi) damaging DNA [7]. The teratogenicity of VPA mostly is found in genetic and somatic levels [7]. Folate deficiency elicits hyperhomocysteinemia, which has been considered a mediator of the teratogenic potential of VPA [1, 6, 8], including neural tubular defect (NTD) and spina bifida aperta [9]. Supplementation with maternal folate greatly decreased the risk [10]. However, the role of folate playing in NTD risk is not well defined [11]. A diversity of nutrients and nutraceuticals have been tried to prevent or antagonize VPA-related teratogenicity [1]. However, the protective efficiency was very limited. NTDs develop during the gestation are due to combination of genetic and

environmental causes (multifactorial). In physiological state of hyperglycemia (>250 mg/dL) plus hypoxia (12% O₂), *pax-3* gene expression decreased five folds, and as consequence the incidence of NTD increased eight folds [2]. Nonetheless, the genetic causes induced by VPA are largely unknown [12] previously, using the chicken embryo model (CEM) we showed folate greatly improved many defects caused by VPA [1]. We hypothesize that VPA might alter the expression of some relevantly related genes including folate receptor (*folr1*) and *pax-3* in the earlier embryonic stage. To verify this, we conducted the experiments using the CEM. In addition, microarray GeneGO analysis and qPCR were applied to investigate the related genes. VPA induced strong oxidative stress [4] and homocysteine accumulation [1]. While N-acetylcysteine (NAC) was able to supply extra cysteine source and simultaneously afford promising antioxidative activity [13]. For alleviation, NAC was commenced to suppress the adverse effects of VPA.

Materials and Methods

Chemicals

Valproic acid (VPA), N-acetyl-L-cysteine (NAC), agarose, homocysteine, folic acid, fluorobenzofurazan-4-sulfonic acid ammonium salt (SBD-F), fast green dye were provided by Sigma Aldrich Co. (St. Louis, MO, USA). dNTP, and poly-A primer, random primer were purchased from Biobasic (Canada). GenTaq DNA Polymerase, M-MuLV Reverse Transcriptase, 50×TAE and Total RNA Miniprep Purification Kit were supplied by Jane-Mike Biotech Co. (Taichung, Taiwan). Light Cycler SYBR I master was a product of Roche Pharmaceuticals (Switzerland). Chicken genome array involving *RGS4* oligonucleotide, *EDNRB* oligonucleotide, *COL6A3* oligonucleotide, *NAPDH* oligonucleotide, *KLF6* oligonucleotide, *IGF2R* oligonucleotide, *FOLR1* oligonucleotide, and *PAX-3* oligonucleotide was provided by Affymetrix Co. (USA).

Source of fertilized eggs and processing

This experimental protocol was approved by the National Changhua University of Education Ethic Committee of Experimental Animals (Changhua, Taiwan). Day-1 fertilized Leghorn eggs were supplied by Qing-Dang Chicken Farm (Taichung, Taiwan). The experiment was conducted in two parts. The first part was carried out to test the optimum dose of VPA. The second part was conducted to test the protective effect of NAC at two level doses, 10 mM and 20 mM [1]. In the first part, 48 day-1 fertilized eggs were divided into four groups, each 12 eggs: PBS control, VPA 10 mM, 20 mM, and 30 mM (translated to 2.89, 5.77, and 8.66 mg/kg; or 20, 40, and 60 µM final tissue concentrations). The fertilized eggs were placed in an incubator (Haw-Yang Agricultural Farm, Taichung, Taiwan) and incubated at 37°C, RH 55–65% for further 1.5 days. The day-2.5 fertilized eggs were moved to a laminar flow chamber. A hole having size 2×2 mm on the egg shell was aseptically drilled through with a hole-driller. The embryos were gently moved as close as to the hole opening by carefully turning around in between the observer's eyes and a direct strong light source. An amount of 100 µL VPA was injected with a tip injector to sites as near as

possible to the yolks. The openings were aseptically sealed with a 3M tape. The incubation was continued. On day 21, the chicks were examined for their normal, still birth, and malformation rates. The second part of experiment was carried out with 72 fertilized eggs. These eggs were grouped into PBS (negative) control, VPA 30 mM, NAC 10 mM (NAC 10 mM, 100 µL/egg, to give a final concentration of 3.3 µg/kg), NAC 20 mM (NAC 20 mM, 100 µL/egg, to give a final concentration of 6.6 µg/kg), VPA (30 mM) + NAC (10 mM), and VPA (30 mM) + NAC (20 mM), each 12 eggs. Similar procedures were conducted as mentioned in the above. On day-2.5, the test solutions (each 100 µL) were applied. The openings were aseptically sealed with a 3M tape. The incubation was continued. The sampling points were set at HH stage 22 (day-3.5 embryo).

Determination of vascularization and vessel density

The HH stage 22 (day-3.5)-embryos were carefully removed off their chorioallantoic membranes, blood vessel, yolk and egg white. The embryo was successively rinsed with several times with PBS and deionized water (dw). The embryos were transferred onto a glass plate, 1 mL of fast green dye was added. After one minute, the photos of the vascularization status and embryos were taken with an anatomical real image microscope (Type Castor BI-90A, Luminescence/UV Image system). The extent of vascularization were taken and analyzed with Image-Pro Plus 6.0 software. The other intact embryos were stored at -80°C for further use.

Blood and tissue sample collection

The HH stage 46 (day-1)-chicks were bled from heart to collect the blood sample. After blood collection was finished, the chicks were euthanized immediately with CO₂. The cervical muscles were collected, rinsed with PBS and dewatered with tissues. After the picture of excised cervical muscles were taken to examine the pathological changes of outer appearance, the organs were separately dipped into 10% buffered neutral formalin at a ratio 1:30 for 48 hours to proceed paraffin-embedding preparation.

Histopathological examination

The somites of embryos were collected, carefully rinsed with PBS, dried on fine tissues, and dipped into 10% buffered neutral formalin at a volume ratio 1:30 for 48 hours to proceed paraffin embedding preparation. The paraffin-embedded slides were subjected to HE staining, and the slides were observed with Castor BI-90A Microscope (Luminescence/UV Image system).

HPLC analysis for serum folic acid level

Serum folic acid level was determined according to the method previously described [1]. Hitachi HPLC equipped with RP-18 GP 250-4.6 (5 mm) column, L-2100/2130 pump, and L2485 fluorescence detector (Hitachi High Tech, Tokyo, Japan) was used. Briefly, 60 µL of serum sample was mixed with 180 µL of solution A, and the remaining procedure was conducted as previously cited [1]. The fluorescence intensity of the final solution was read with an ELISA Fluorescence

Reader at $\lambda_{\text{ex}}=250$ nm and $\lambda_{\text{em}}=350$ nm. Same volume (20 μL) of authentic folic acid solution was similarly treated to establish the calibration curve within concentration range 6.25 to 200 μM .

HPLC analysis for serum homocysteine (s-Hcy) level

Hitachi HPLC L-2100/2130 type (Hitachi High Tech, Tokyo, Japan) equipped with L-2100/2130 pump and L2485 fluorescence detector was used to determine serum homocysteine level as previously described [1].

Briefly, to the serum sample (60 μL) and equal volume of authentic homocysteine solution (60 μM), 39 μL Dulbecco's phosphate buffered saline and 10 μL TECP were added and the mixture was left to react at ambient temperature for 30 minutes. The following protocols were carried out similarly as described [1]. The fluorescence was read at $\lambda_{\text{ex}}=385$ nm and $\lambda_{\text{em}}=515$ nm. A calibration curve was established using authentic homocysteine solution at concentrations 3.75, 7.5, 15.0, 30.0, and 60.0 μM similarly treated by the same procedure as mentioned.

Assay for tissue histone deacetylase (HDAC) level

The activity of tissue histone deacetylase was determined as previously described [1]. In brief, to embryonic tissue (100 mg) 0.5 mL cold lysis buffer (pH 7.5, containing 10 mM Tris-HCl, 10 mM sodium chloride, 15 mM magnesium chloride, 250 mM sucrose, 0.5% Triton-X100, and 0.1 mM EGTA) was added and homogenized. The following procedures were similarly conducted [1]. The fluorescence intensity of the final solution was read with an ELISA Fluorescence Reader at $\lambda_{\text{ex}}=340\text{--}360$ nm and $\lambda_{\text{em}}=440\text{--}460$ nm. The calibration curve was also similarly established using the deacetylated histone standard (2.1 mM) at 10-fold dilution, from which the amount of HDAC was calculated.

Quantitative Polymerase Chain Reaction (qPCR)

RNA extraction

Following the instructions given by TriReagent kit, the frozen (-80°C) embryonic tissue (100 mg) was precisely measured and 1 mL of TriReagent (Sigma, Poole, England) was added. The mixture was homogenized with a hand portable homogenizer (No. 985370, Ekso Biotech Co., Taichung, Taiwan) for 10 minutes and left to stand for five minutes to facilitate the separation of nucleoprotein.

To the mixture, 0.2 mL of chloroform was added and agitated vigorously for 15 seconds. The mixture was left to stand at ambient temperature for 2–3 minutes and then centrifuged at $12\,000\times g$ at 4°C for 15 minutes. The mixture at this point would appear in three layers: the phenol chloroform layer (at the bottom), the middle layer, and the upper layer (colorless aqueous layer). The upper layer containing RNA (0.6 mL) was removed out by a micropipette and transferred to a centrifuge tube

containing 1.0 mL of TriReagent. To the mixture, isopropanol (0.25 mL) and PS & PG Removal Solution (0.25 mL) were added, mixed well and left to stand for 10 minutes at the ambient temperature. The mixture was centrifuged at $12\,000\times g$ at 4°C , for 10 minutes, and the supernatant was removed. To each mL of TriReagent 1 mL of ethanol (75%) was used to rinse the RNA pellets. The same rinsing procedure was repeated for once again. Each time the RNA pellets were subject to vortex and centrifuged at $12\,000\times g$ at 4°C for 5 minutes. The ethanol rinsing solution was removed. The RNA pellets were air-dried for 5–10 minutes. The dried RNA pellets were redissolved with water previously treated with diethyl-pyrocabonate (DEPC, 25 μL). The optical density (OD) was measured with the Nano-Drop 1000 Spectrophotometer (Thermo Fisher Scientific Inc., Waltham, MA, USA). The value of OD ratio A_{260}/A_{280} ($=1.7\text{--}2.1$) was used to evaluate the extraction efficiency. The product RNA was refrigerated at -80°C for further use (sample RNA).

The Reverse Transcription Polymerase Chain Reaction (RT-PCR)

The RNA content of the sample RNA was measured with the Nano-Drop 1000 Spectrophotometer (Thermo Fisher Scientific Inc., Waltham, MA, USA). All RNAs were synchronized to the same concentration and the RT-PCR was conducted to prepare the cDNA. Briefly, the reaction system contained RNA 4.5 μL , Oligo dT primer 4.5 μL , random primer 1 μL , and DEPC water 1 μL to make a total of 11 μL . The mixture was heated at 70°C in a dry bath for 5 minutes and then immediately cooled on ice for 3 minutes. To the ice-cooled mixture, MMLV buffer ($10\times$) 2 μL , dNTP (10 mM) 1 μL , MMLV reverse transcriptase 1 μL , and DEPC water 5 μL were added to make a total of 20 μL . PCR was conducted according to the specified condition for each specific gene as given by the manufacture. The OD of the mixture was measured and the OD ratio A_{260}/A_{280} was calculated. The range within $1.7\text{--}2.1$ was preferred. The preparation was frozen at -20°C for use.

PCR for genes folate receptor (*folr1*) and *pax-3*

The PCR was conducted to analyze the expression of *pax-3* and *folr1* genes in day 3.5- and day 5.5-chicken embryos. Briefly, the Gene Marker PCR Kits (Roche LightCycler[®] 2.0 Instrument, Taichung, Taiwan) were used for this analysis. The kits contained cDNA (500 ng/ μL) 3 μL , GeneTaq polymerase 1 μL , GeneTaq buffer 2.5 μL , Forward Primer (5 μM) 0.75 μL , Reverse Primer (5 μM) 0.75 μL , ddH₂O 15.5 μL , and dNTP 1.5 μL , to make a total of 25 μL . The temperature was programmed as: pre-denaturation at 94°C for three minutes; denaturation at 94°C for 30 seconds; annealing at 58°C for 30 seconds for *folr1* gene or at 63°C for 30 seconds for *pax-3* gene; extension at 72°C for 45 seconds; final extension at 72°C for three minutes, and finally for cool-down at 20°C for two minutes. The primers used were highlighted in Table 1.

Table 1 – The primers used for PCR

| Gene | Forward | Reverse |
|--------------|--------------------------|----------------------------|
| <i>Folr1</i> | TGCTGCACGGCCAACAC | TGGTTCCAGTTGAAGTTGTACAGGTA |
| <i>Pax-3</i> | GCATCCGGCCCTGTGTCTCATCTC | GCTCCTGCCTGCTTCTCTCCATCT |

The DNA agarose electrophoresis

Agarose was dissolved in 5×TAE buffer to attain a concentration of 0.8 to 1.5%. The agarose in 5×TAE buffer was heated by microwave until completely transparent without any contaminants appearing in sights. To the solution 3 µL of the internal dyeing agent safe view DNA stain/100 mL were added. The solution was left to cool down at ambient temperature. After 10 minutes, the solution was poured into the casing pan, and the gas bubbles were driven off during the operation. The agarose was allowed to solidify at the ambient temperature, avoiding the direct sunlight. The finished agarose was placed into the electrophoresis chamber in which 5×TAE buffer was filled up to serve the electrophoresis buffer. A total amount of DNA (100 ng), mixed with 6× loading dye, was injected onto the agarose concave, the electrophoresis (DNA Horizontal Electrophoresis Chamber, MJ-105s, Gene Valley, Taichung, Taiwan) was started by applying 100 V potential for 20 minutes. By contrasting with the authentic DNA ladder pattern, the photos of the pattern were taken by the Luminescence/UV Image system and the quantification was subsequently performed.

Microarray analysis

Treatment of fertilized eggs

Similar to the above-mentioned, the day 1 fertilized eggs were incubated in incubator held at 37±1.0°C, RH 50~60% for 1.5 days (HH stage 10). Using similar protocol, VPA (30 mM, 100 µL/egg, final concentration 60 µM) and NAC (10 mM, 100 µL/egg) were applied as indicated. The eggs were further incubated until HH stage 22 (day 3.5) and sacrificed for examination.

RNA purification

The procedure for RNA purification was conducted according to the instructions issued by the Total RNA Miniprep Purification Kit (Gene Marker, Taichung Taiwan). The RNA obtained was amplified with PCR (Thermo electron Px2 Thermal Cycle, Gene Valley, Taichung, Taiwan) to 500 ng, the cRNA obtained was fluorescence-labeled with the Affymetrix GeneChip 3'IVT Express Kit.

Microarray hybridization

The hybridization solution and Affymetrix oligonucleotide microarrays were left to react at 45°C for 10 minutes at 65 rpm. The pre-hybridization solution was removed, and 200 µL of hybridization solution containing 0.05 µg/µL fragmented cRNA was added. The mixture was left to react at 45°C for 16 hours at a revolution speed of 65 rpm. The Affymetrix GeneChip® Scanner 3000 was used to scan the chips. For each sample, repeated microarray hybridization was carried out six times.

Normalization and filtering

After the image files (Cel) were developed by the Affymetrix gene chips operation software (GCOS), the dChip software invariant set was used to normalize the data [14]. All the chips use to participate the analytical work were examined and the strength of the median chip was selected to act as the baseline strength. In addition, the others were normalized against this median data. The variance among the groups detected by the completely

compensating probe (PM) was used as the basis to simulate the normalized curve. Moreover, from the normalized data revealed by the chip the fold change, the difference, and the *t*-test *p*-value among the groups were calculated. Herein we were interested only in the significance with (i) a fold change >3.0 (or <-3.0); (ii) a difference >100; and (iii) a *p*-value <0.05.

Real-time PCR

The real time PCR was conducted by following the manufacturer's instructions given in the Real-Time PCR/SYBR Green flow chart using the LightCycler® RNA Master SYBR Green I Kits (Roche, Taipei, Taiwan).

The entire process was repeated for 50 cycles. To calculate the data, the fluorescent signals detected during the annealing step were measured. The Ct values were calculated. In parallel, the Ct values were estimated by the relative quantification method, which were substituted into the equation $2^{-\Delta Ct}$ to estimate the difference of expression in the target gene between the treated and the control groups. For each sample, qPCR was repeated for six times.

Statistical analysis

The data obtained were analyzed with the Statistical Analysis System 9.0 (SAS 9.0) and expressed in mean ± SD. The variance between groups was analyzed using ANOVA Test. A level of *p*<0.05 was set as the confidence level.

Results

VPA (30 mM, 100 µL/egg) was optimum for inducing the malformation rate. NAC was only partially effective in rescuing the malformation rates

VPA induced malformation in a dose responsive manner. The malformation rate was 17±8%, 20±8% and 29±13%, respectively at 10, 20 and 30 mM (each 100 µL/egg) (Table 2), consistent with our previous report [1], among which 30 mM (each 100 µL/egg) was optimum for induction of the malformation in CEM.

Table 2 – Dose responsive effect of VPA, NAC, and the protective effect of NAC in VPA+NAC groups on the malformation rate in CEM

| Group | Normal [%] | Still birth [%] | Malformation rate [%] |
|-------------|----------------------|----------------------|-----------------------|
| PBS control | 95±8 ^{a,A} | 5±2 ^{c,D} | 0.0 ^{f,E} |
| VPA | — | — | — |
| 10 mM | 83±13 ^b | 0.0 ^d | 17±8 ^c |
| 20 mM | 61±12 ^c | 21±10 ^b | 20±8 ^b |
| 30 mM | 39±5 ^{d,F} | 30±12 ^{a,A} | 29±13 ^{a,A} |
| NAC | — | — | — |
| 10 mM | 82±12 ^{b,C} | 7±4 ^{c,D} | 12±6 ^{d,C} |
| 20 mM | 87±11 ^{b,B} | 6±4 ^{c,D} | 7±3 ^{e,D} |
| VPA 30 mM | — | — | — |
| + NAC 10 mM | 58±14 ^E | 24±7 ^B | 18±8 ^B |
| + NAC 20 mM | 67±11 ^D | 20±5 ^C | 13±5 ^C |

*Values with different superscripts in lower cases in the same column indicate significantly different between groups exclusive of the treated (*p*<0.05). Values with different superscripts in upper cases in the same column indicate significantly different when compared to the treated group (the bottom three lines) (*p*<0.05).

Unless otherwise stated, this dose was adopted to perform the subsequent experiments. NAC at 10 and 20 mM (each 100 µL/egg) significantly suppressed in a dose responsive manner the malformation rate down to

18±8% and 13±5%, and the still birth rates down to 24±7% and 20±5%, respectively (Table 2).

NAC completely alleviated the dysvascularization induced by VPA

The vascular density and neural tube was highly affected

by VPA 30 mM (each 100 µL/egg) (Figure 1, A and C). In HH stage 22 (day 3.5) CEM, VPA at 10, 20, and 30 mM suppressed the vascularization area to 6.0, 5.2, and 4.0% in a dose responsive manner compared to normal value 6.4±2.5% (Figure 1B).

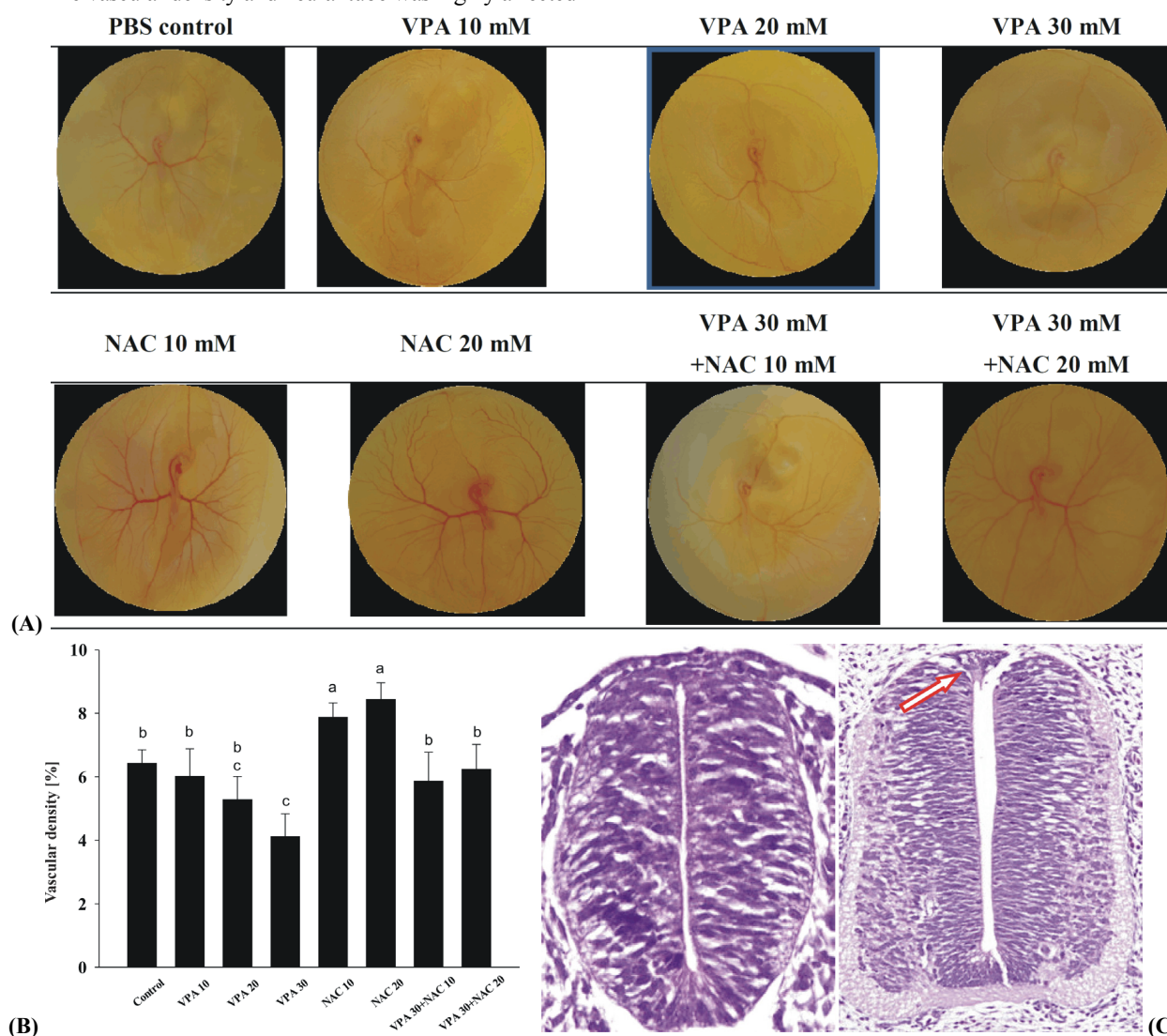


Figure 1 – Physiopathological changes in HH stage 22 (day 3.5)-chicken embryos after treated with valproic acid (VPA) and N-acetylcysteine (NAC). Status of vascularization (A); vascular density (B); and the light micrographs of Hematoxylin–Eosin stained somite showing incomplete closure of somite induced by VPA (C). Valproic acid (VPA, 30 mM, 100 µL/egg, translated to 60 µM or 8.66 mg/kg). N-acetylcysteine, NAC (10 or 20 mM, each 100 µL/egg, corresponding to 3.3 and 6.6 µg/kg respectively). The HE stained somites (×200) of the PBS control (left) and VPA treated (right) (C). Each value in (B) represents mean ± SD from triplicates (n=12). Different letters indicate significantly different (p<0.05).

NAC completely restored the VPA inhibited-HDAC

Administration of VPA (30 mM, each 100 µL/egg)) suppressed the HDAC level to 0.9±0.2 nmol/min./mg protein, which was significantly lower than the normal 3.9±0.2 nmol/min./mg protein. The inhibition reached – 51% (p<0.001) and was effectively restored by NAC at 20 mM (Figure 2).

NAC completely alleviated homocysteine accumulation but folate deficiency was only ameliorated at higher doses of NAC

HPLC analysis showed folate and homocysteine

to exhibit retention times 2.63 min. (Figure 3A) and 13.41 min. (Figure 3B), respectively. The control-serum folate level was 98 µM. VPA induced significant folate deficiency (-17.4%, 81 µM), which was ameliorated by NAC at 20 mM to 132 µM (+34.7%) (Figure 3, C and D).

VPA downregulated genes folate receptor *folr1* and *pax-3*

The folate receptor gene (*folr1*) in HH stage 22 (day 3.5) CEM was downregulated in a dose-responsive manner by 10, 20 and 30 mM of VPA (each 100 µL/egg). Day 3.5 CEM was more susceptible to VPA showing sensitivity 1.60 folds/µM folic acid. NAC failed to retard such downregulation (Figure 4A), much less susceptible for day

5.5 CEM (Figure 4B): the *folr1* gene was downregulated in a dose responsive manner to 0.91, 0.84 and 0.61 folds that of control (Figure 4B). The susceptibility was reduced to only 0.80 folds/ μ M folic acid, implicating the higher susceptibility of the earlier embryonic stage to VPA. As contrast, *pax-3* gene in HH-stage 22 (day 3.5) CEM seemed to be totally unaffected by VPA therapy and NAC supplement (Figure 5).

Microarray analysis – GeneGo analysis

Microarray analysis revealed a total of 21 genes were affected when administered VPA (30 mM, 100 μ L/egg), 17 downregulated and four upregulated (Figure 6A, Table 3). GeneGo analysis showed five genes were closely intermodulating each other, they were (gene, fold change): insulin-like growth factor 2 receptor gene (*IGF2R*, -3.43), regulator of G-protein signaling 4 gene (*RGS4*, -3.97), alpha 3 (VI) collagen gene (*COL6A3*, -3.55), endothelin receptor type b gene (*EDNRB*, -3.44), and Krüppel-like factor 6 gene (*KLF6*, -3.51) (Table 3). We suspected that these five genes could be closely related to NTD, hence qPCR was further conducted. Quantitatively, the two results were rather matching (Figure 6B).

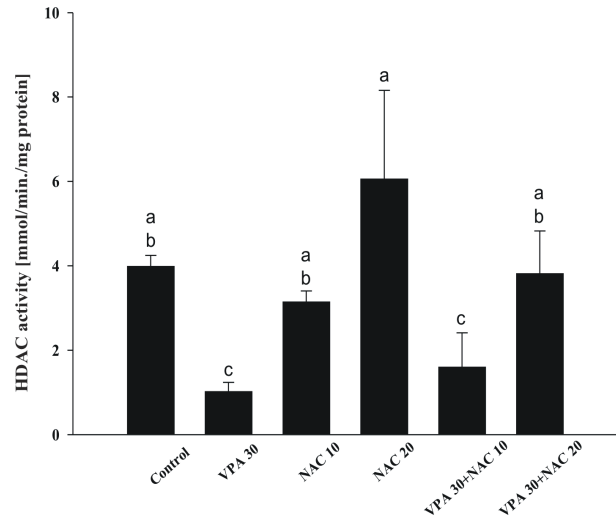


Figure 2 – Change of tissue histone deacetylase (HDAC) activity in HH stage 22 (day 3.5)-chicken embryos after treated with VPA and NAC. Each value represents mean \pm SD (n=12). Different letters indicate significantly different ($p < 0.05$).

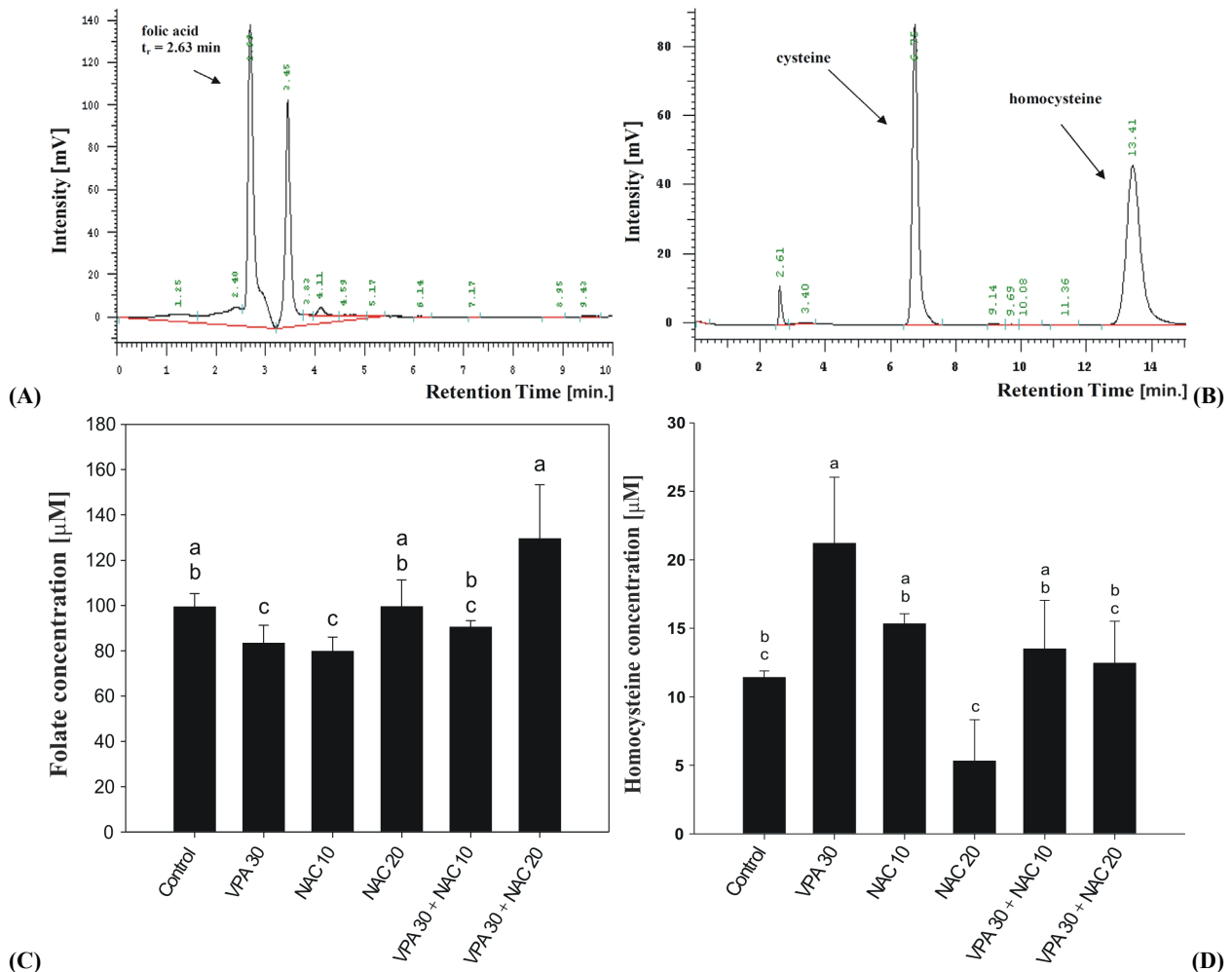


Figure 3 – HPLC determination for serum folic acid (A) and homocysteine (B). Folate deficiency (C) and the homocysteine accumulation (D) in the valproic acid treated HH stage 22 (day 3.5)-chicken embryos. Conditions for performing HPLC are presented in the text. The retention time (RT) is 2.63 min. for folate, 13.41 min. for homocysteine, and 6.75 min. for cysteine.

Figure 4 – *Folr1* gene in HH stage 22 (day 3.5)-chicken embryos affected by VPA and NAC was analyzed by semi-quantitative reverse transcriptase polymerase chain reaction (RT-PCR). Its expression levels were normalized with glyceraldehyde-3-phosphate dehydrogenase housekeeping gene levels (A). Comparison of the expression of *Folr1* gene between day 3.5- and day 5.5-chicken embryos (B). Each value represents mean \pm SD (n=12). Different letters indicate significantly different ($p<0.05$).

Figure 6 – Genomic analysis. The microarray GeneGO analysis revealed 21 genes in HH stage 22 (day 3.5)-chicken embryos were apparently affected by VPA therapy (A). A comparison of microarray and qPCR (B). VPA (30 mM, 100 μ L/egg, translated to human = 8.66 mg/kg) or NAC (10 mM, 100 μ L/egg).

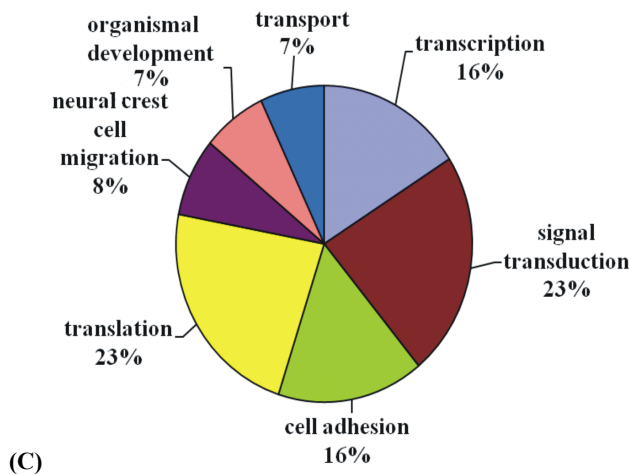


Figure 6 (continued) – Genomic analysis. The pie diagram showing the proportion of biological significance (C). VPA (30 mM, 100 μ L/egg, translated to human = 8.66 mg/kg) or NAC (10 mM, 100 μ L/egg).

(C)

Table 3 – Microarray analysis of genes in HH stage 22 (day 3.5) chicken embryos transcriptionally expressed in respond to VPA treatment^a

| Representative public ID | Symbol | Name of gene | Fold change |
|--------------------------|--------------|---|-------------|
| NM_204970.1 | IGF2R | Insulin-like growth factor 2 receptor | -3.43 |
| NM_204118.1 | AHR | Aryl hydrocarbon receptor | -2.27 |
| NM_204385.1 | RGS4 | Regulator of G-protein signaling 4 | -3.97 |
| NM_205534.1 | COL6A3 | Collagen, type VI, alpha 3 | -3.55 |
| NM_205115.1 | LIMK2 | LIM domain kinase 2 | -1.36 |
| NM_001001744.1 | IRX4 | Iroquois homeobox 4 | 1.34 |
| AJ720222 | ACAP2 | ArfGAP with coiled-coil, ankyrin repeat and PH domains 2 | -1.42 |
| BU253126 | LOC771075 | Hypothetical protein LOC771075 | -1.8 |
| BU199767 | LOC426092 | Hypothetical gene supported by CR386914 | 1.28 |
| BU449947 | EDNRB | Endothelin receptor type B | -1.32 |
| BX932265.1 | EDNRB | Endothelin receptor type B | -3.44 |
| CR353052.1 | VPS26B | Vacuolar protein sorting 26 homolog B (<i>Schizosaccharomyces pombe</i>) | 2.1 |
| AF317286.1 | LOC395379 | Ephrin-A6 | -1.35 |
| AJ720905 | KLF6 | Kruppel-like factor 6 | -3.51 |
| ENSALT00000016072.1 | C1orf107 | Chromosome 1 open reading frame 107 | 2.17 |
| AJ720126 | RMND5A | Required for meiotic nuclear division 5 homolog A (<i>Saccharomyces cerevisiae</i>) | -1.32 |
| ENSALT00000008340.1 | LOC424460 | Hypothetical LOC424460 | -1.9 |
| ENSALT00000011854.1 | RCJMB04_2I20 | LIM domain containing preferred translocation partner in lipoma | -5.65 |
| BX273571 | CASK | Calcium/calmodulin-dependent serine protein kinase (MAGUK family) | -1.52 |
| BU480610 | TMEM184B | Transmembrane protein 184B | -1.29 |
| CD732748 | LEMD2 | LEM domain containing 2 | -2.48 |

^aValproic acid (VPA) 8.66 mg/kg (= 60 μ M; VPA 30 mM, 100 μ L/egg) alone was applied to fertilized chicken embryo using the protocol stated in the text. Microarray analysis revealed a total of 21 genes affected when administered VPA 30 mM: 17 downregulated and four upregulated (also see Figure 5).

Discussion

The VPA-induced malformation was not only simply due to the homocysteine accumulation and oxidative stress

VPA induced malformation in a dose responsive manner. At 30 mM (100 μ L/egg), the malformation reached maximum with the least mortality, hence for investigation of the teratogenicity of VPA, we adopted this dose. VPA induced strong oxidative stress [4] and homocysteine accumulation [1]. As mentioned, NAC had been shown able to supply extra cysteine source and simultaneously afford promising antioxidative activity [13]. Nonetheless, we showed NAC to be only partially effective in the alleviation of malformation, underlying the complicate etiology of VPA-induced malformation.

Hyperhomocysteinemia is a major mediator of the teratogenic potential [1, 6] and an extremely important risk factor for the neural tubular defect (NTD) [9]. Nonetheless, the prevalence of NTD is independent of the ambient folate concentration, acting directly on embryonic development or indirectly through methionine cycle [1, 15].

Regarding the teratogenicity of VPA, Rosenquist TH and Finnell RH (2001) suggested three general families of genes to be considered: the gene folate-receptor; genes regulating methionine–homocysteine metabolism; and gene NMDA-receptor [16].

VPA induced metahypoxic state with subsequent mitochondrial dysfunction

The vascular density was highly reduced by VPA.

Assume the vascularization density to be positively proportional to the oxygen transport, the corresponding decrease in oxygenation rate could have reached -6.3%, -18.8%, and -37.5%. A decrease of -37.5% in oxygenation rate implied a metahypoxic state having 13.2% atmospheric oxygen (Figure 1B), consistent with Rosenberg G (2007) study [6]. Worth note, accelerated glucose consumption and metabolism could also increase the demand for oxygen, and dysvascularization status would have further exacerbated the hypoxic state [2].

NAC increased the vascular density to 7.9 and 8.4% at 10 and 20 mM ($p < 0.05$) (Figure 1B), counteracting VPA and completely alleviating the vascularization ($p < 0.05$) (Figure 1B), suggesting the fact VPA induced NTD through dysvascularization and mitochondrial dysfunction (Figure 1C), consistent with Nanau RM and Neuman MG (2013) study [15].

NAC effectively rescued HDAC activity to retard the teratogenicity of VPA

Administration of VPA (30 mM each 100 μ L/egg) severely suppressed the HDAC, yielding a suppression of -51% ($p < 0.001$) (Figure 2). Literature indicated an increase of six-fold histone H3 acetylation was approached when treated with VPA [17, 18]. Phiel CJ *et al.* demonstrated VPA (5 mM) downregulated nuclear HDAC activity by 77% [19], similar results had been demonstrated by Hsieh CL *et al.* (2012) [1].

Although *in vivo*, only up to 20% of the whole genome is controlled by HDACs, key processes for development, survival, proliferation, and differentiation have been strictly linked to HDAC enzyme functioning [20]. To date, all tested HDACi have shown teratogenic effects similar to those described for VPA in many animal models [1, 7].

NAC at 20 mM alone increased the activity of HDAC to 6.0 nmol/min./mg protein, reaching 1.54-fold that of the control. Previously, we showed NAC at 10 mM effectively rescued the VPA induced-downregulation of HDAC in day 5.5 CEM [1], implicating embryos at earlier stage to be more susceptible to VPA.

Why external folate could completely rescue the malformation induced by VPA even when the folate receptor gene, *folr1* was severely downregulated?

In previous report, we showed externally supplemented folic acid effectively ameliorated the malformation of chicken embryos [1]. The question arises “Why the externally supplemented folate could exert such a full strength anti-folate-deficiency under circumstance when *folr1* was suppressed by -47% by 30 mM VPA (Figure 4B)?”

The reason is that the cells use multiple strategies to assimilate folate, *e.g.* (i) the GPI-linked folate receptors (MFRs) on the cell surface bind folate and deliver it to an endosomal compartment through receptor-mediated endocytosis pathways that are not fully understood. MFRs have high affinities for folic acid (K_d 0.1 nM^{-1}) and reduced folate (K_d 0.1–10 nM^{-1}) [21]; (ii) the reduced folates can enter the cell through a facilitative carrier (SLC19A1)-mediated mechanism, which exhibits features of anion exchangers (RFC) [22]; and (iii) the proton-

coupled folate transporter (PCFT) recently identified as SLC46A1 [23], which is necessary for normal intestinal absorption of dietary folate. Consequently, even when folate deficiency occurred due to simply impaired folate receptor (FR), its effect would not be easily perceived, because the other pathways could be adequately working instead of FR.

Why *pax-3* gene was not affected?

Pax-3 gene in HH-stage 22 (day 3.5)-CEM seemed to be totally unaffected by VPA therapy and NAC supplement (Figure 5). The reason could be due to the incomplete hypoxic state in the CEM. Oxidative stress could inhibit expression of genes, such as *pax-3*, which control essential developmental processes and embryopathy [24]. Alternatively, in physiological state of hyperglycemia (>250 mg/dL) plus hypoxia (12% O_2), *pax-3* gene expression can be decreased up to five folds, and as consequence the incidence of NTD increased eight folds [2]. When the atmospheric O_2 tension was increased to 30%, the maternal diabetes-directed NTD was significantly suppressed [2].

Pax-3 protein is required during neural tube development to suppress p53-dependent cell death and consequent abortion of neural tube closure, but is not required to control expression of genes that direct neural tube closure [24].

Literature elsewhere indicated in VPA-exposed embryos, some domains were spatially abnormal, for example *pax-3* in the neural crest [25]. Suggestively, even VPA caused dysvascularization (Figure 1), which might merely have induced a state of metahypoxia. Hence, *pax-3* gene was unaffected (Figure 5).

Microarray analysis supported the linking of hypoxia, dysvascularization and neural tube defect, and simultaneously the overall promising ameliorating effect of NAC

Downregulation of *IGF2R* could enhance dysvascularization (Figure 1B) associated with hypoxia [24]. As well known, *RGS4* is one of the major modulator of G-protein signaling, which is associated with a diversity of *in vivo* pharmacological action mechanisms of drugs [26]. *RGS* genes have been identified to act as novel regulators of the G-protein-coupled receptor signaling [27]. *Alpha 3 (VI) collagen (COL6A3)* gene provides instructions for making one component of type VI collagen, a flexible protein that surrounds muscle cells. Type VI collagen networks play an especially important role in the extracellular matrix of muscle that is used for movement (skeletal muscle) (*Genetic Home References: Reviewed October 2010*). *EDNRB* gene provides instructions for making a protein called endothelin receptor type B, a G-protein-coupled receptor that activates a phosphatidylinositol-calcium second messenger system [28]. The receptor–ligand interacts to regulate several critical biological processes, including the development and function of blood vessels (*Genetics Home Reference, Reviewed April 2006*), which may also be associated with dysvascularization. A mutation in the middle of the *EDNRB* gene leads to undeveloped embryos and non-migrating enteric neuron precursors [28]. Krüppel-like

factor (KLF) *klf6* gene is expressed in developing neuronal tissues [29, 30], which implied the linking to the neural tube defect. The *klf6*^{-/-} mutation causes embryonic lethal associated with markedly reduced hematopoiesis and poorly organized yolk sac vascularization [29]. *LOC426827* gene is highly expressed in brain, bone marrow, small intestine, muscle, spleen and pancreas [31]. *C1orf107* gene plays a structural role at sites of cell adhesion in maintaining cell shape and motility. It is involved in signal

transduction from cell adhesion sites to the nucleus [32]. *RCJMB04_2120* gene plays a structural role at sites of cell adhesion in maintaining cell shape and motility [33]. Worth note, *RCJMB04_2120* gene, once reduced to -5.65 folds when treated with VPA (Table 3) was up-regulated by NAC to -2.92 folds (Table 4). *DIABLO* IAP is a protein that negatively regulates apoptosis or programmed cell death [34], functioning as the second mitochondria-derived activator of caspases or SMAC.

Table 4 – Genes transcriptionally expressed in day HH stage 22 (day 3.5) chicken embryos when treated with VPA+NAC^a

| Representative public ID | Gene symbol | Gene name | Fold change |
|--------------------------|---------------------|--|-------------|
| BU469343 | <i>SEPP1</i> | Selenoprotein P, plasma, 1 | -1.47 |
| BU206830 | <i>DIABLO</i> | Diablo homolog (<i>Drosophila</i>) | -1.31 |
| BU124530 | <i>LOC426827</i> | BTN2A1; DJ3E1.1; BK14H9.1; Butyrophilin BTF1 precursor | -22.53 |
| BX934057.1 | <i>ZCCHC10</i> | Zinc finger, CCHC domain containing 10 | 1.42 |
| AJ719771 | <i>C1orf107</i> | Chromosome 1 open reading frame 107; DEF, DJ434O14.5; Digestive organ expansion factor homolog | -5.31 |
| ENSALT00000011854.1 | <i>RCJMB04_2120</i> | LIM domain containing preferred translocation partner in lipoma | -2.92 |

^aValproic acid (VPA) (VPA 30 mM, 100 µL/egg to achieve 8.66 mg/kg or 60 µM) + N-acetylcysteine (NAC) (10 mM, 100 µL/egg to achieve a final concentration 3.3 µg/kg) were applied to fertilized chicken embryo using the protocol stated in the text. Microarray analysis revealed only six genes were affected when treated with NAC: five downregulated and one upregulated, evidencing that NAC had partially rescued, if not entirely, the teratogenicity of VPA (also see Figure 5).

In addition, the *Gene Ontology Biology Process Analysis* revealed the biological significance of these gene alterations, which involved 23% translation, 23% signal transduction, 16% transcription, 16% cell adhesion, 8% neural cell migration, 7% transport, and 7% organismal development (Figure 6C). When treated with NAC (10 mM) [1], only six genes remained to be significantly affected: five downregulated and one upregulated (Table 4). *SEPP1* (Selenoprotein P) gene normally signals translation termination and also has been implicated to function as an antioxidant in the extracellular space [35]. *DIABLO* gene encodes an inhibitor of apoptosis protein (IAP)-binding protein. The encoded mitochondrial protein enters the cytosol when cells undergo apoptosis, and it moderates the caspase inhibition of IAPs. *DIABLO* promotes apoptosis by activating caspases in the cytochrome c/Apaf-1/caspase-9 pathway. *DIABLO* acts by opposing the inhibitory activity of inhibitor of apoptosis proteins (IAP) (*Genetics Home Reference*). *LOC426827* (*BTN2A*) gene mRNA is expressed in most human tissues but protein expression is significantly lower in leukocytes. Moreover, a particular glycosylated form of *BTN2A1* binds a lectin molecule, DC-SIGN, found on DCs, confirming the involvement of the BTN family as co-regulators of the immune system [36]. *ZCCHC10* widely expressed in normal tissues and systems involving immune, nervous, muscle, internal organ, and secretory glands (*Weismann Institute of Science*). These three genes were only slightly downregulated by VPA+NAC (Table 4). Interestingly, *LOC426827* (*BTN2A*) gene was severely downregulated -22.53 folds (Table 4). The highly downregulated *LOC426827* (*BTN2A*) implicated the severe defect in immune system when treated with VPA that was incurable by NAC. On the other hand, the VPA-upregulated *C1orf107* gene (Table 3) was effectively rescued by NAC (Table 4). Similar phenomenon was found for *RCJMB04_2120* gene (Tables 3 and 4).

A summarized gene expressions relevantly associated with VPA induced-NTD and the alleviation by NAC are shown in Figure 7.

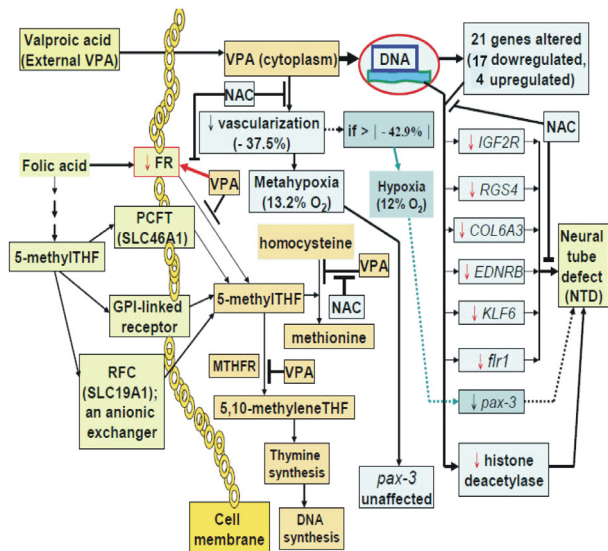


Figure 7 – The genes significantly altered by VPA in the chicken embryo model. Twenty-one genes were significantly altered by VPA therapy: 17 downregulated and four upregulated. Among these, the genes mostly relevant to neural tube defect are *JGF2R*, *RGS4*, *COL6A3*, *EDNRB*, and *KLF6*. Folate receptor gene (*folr1*) was significantly downregulated by VPA (30 mM, 100 µL/egg, translated to 60 µM or 8.66 mg/kg). However, the externally supplement folic acid in form of reduced folates still will be available in cytoplasm. The extra-transport through cell membrane can take three subsidiary routes: the reduced folate carrier (RFC, *SLC19A1*), the GPI-linked membrane folate receptor (MFR), and the proton-coupled folate transporter (PCFT, *SLC46A1*). The cytoplasmic VPA induced dysvascularization, creating a status of meta-hypoxic state (-37.5% of oxygen supply, corresponding to 13.1% of O₂), hence the *pax-3* gene was unaffected. Literature indicated that *pax-3* gene was downregulated under hypoxic state (at 12% O₂ or -43% of oxygen supply). VPA inhibited the conversion of homocysteine into methionine, resulting homocysteine accumulation. VPA also inhibits the methyltetrahydrofolate reductase (*MTHFR*), compromising DNA de novo synthesis.

Conclusions

VPA affects 21 genes: 17 downregulated and four upregulated. Among which, *IGF2R*, *RGS4*, *COL6A3*, *EDNRB*, and *KLF6* genes are apparently intermodulating and supposed to be relevantly related to the prevalence of NTD. In addition, VPA dose responsively downregulates gene *folr1* but to a slight extent on *pax-3* gene. These adverse effects can be only partially alleviated by N-acetylcysteine.

Acknowledgments

The authors are grateful for financial support from the National Science Council NSC 101-2320-B-038-030, NSC 102-2313-B-018-001-MY3, and NSC 102-2320-B-038-025. We also want to show our thanks to the technical assistance for performing HPLC analysis of Mr. Jia-Ping Deng.

References

- [1] Hsieh CL, Wang HE, Tsai WJ, Peng CC, Peng RY, *Multiple point action mechanism of valproic acid-teratogenicity alleviated by folic acid, vitamin C, and N-acetylcysteine in chicken embryo model*, Toxicology, 2012, 291(1–3):32–42.
- [2] Li R, Chase M, Jung SK, Smith PJ, Loeken MR, *Hypoxic stress in diabetic pregnancy contributes to impaired embryo gene expression and defective development by inducing oxidative stress*, Am J Physiol Endocrinol Metab, 2005, 289(4): E591–E599.
- [3] Roy M, Leclerc D, Wu Q, Gupta S, Kruger WD, Rozen R, *Valproic acid increases expression of methylenetetrahydrofolate reductase (MTHFR) and induces lower teratogenicity in MTHFR deficiency*, J Cell Biochem, 2008, 105(2):467–476.
- [4] Chuang CM, Chang CH, Wang HE, Chen KC, Peng CC, Hsieh CL, Peng RY, *Valproic acid downregulates RBP4 and elicits hypervitaminosis A-teratogenesis – a kinetic analysis on retinol/retinoic acid homeostatic system*, PLoS One, 2012, 7(9):e43692.
- [5] Lheureux PE, Hantson P, *Carnitine in the treatment of valproic acid-induced toxicity*, Clin Toxicol (Phila), 2009, 47(2):101–111.
- [6] Rosenberg G, *The mechanisms of action of valproate in neuropsychiatric disorders: can we see the forest for the trees?* Cell Mol Life Sci, 2007, 64(16):2090–2103.
- [7] Sha K, Winn LM, *Characterization of valproic acid-initiated homologous recombination*, Birth Defects Res B Dev Reprod Toxicol, 2010, 89(2):124–132.
- [8] van Mil NH, Oosterbaan AM, Steegers-Theunissen RP, *Teratogenicity and underlying mechanisms of homocysteine in animal models: a review*, Reprod Toxicol, 2010, 30(4): 520–531.
- [9] Ornoy A, *Valproic acid in pregnancy: how much are we endangering the embryo and fetus?* Reprod Toxicol, 2009, 28(1):1–10.
- [10] Panigrahi I, Kalra J, *Anti-epileptic drug therapy: an overview of foetal effects*, J Indian Med Assoc, 2011, 109(2):108–110.
- [11] O'Byrne MR, Au KS, Northrup H (eds), *Neural tube defects: genetics*, The University of Texas Medical School at Houston, Texas, USA, Published online: 15 Nov 2010.
- [12] Agamanolis DP (ed), *Neuropathology: an illustrated iterative course for medical students and residents. Chapter 11: Congenital abnormalities of the CNS and hydrocephalus*, Akron Children's Hospital, Northeast Ohio Medical University, JAVA Script Code, 2011, 1–5.
- [13] Samuni Y, Goldstein S, Dean OM, Berk M, *The chemistry and biological activities of N-acetylcysteine*, Biochim Biophys Acta, 2013, 1830(8):4117–4129.
- [14] Li C, Wong WH, *Model-based analysis of oligonucleotide arrays: expression index computation and outlier detection*, Proc Natl Acad Sci U S A, 2001, 98(1):31–36.
- [15] Nanau RM, Neuman MG, *Adverse drug reactions induced by valproic acid*, Clin Biochem, 2013, 46(15):1323–1338.
- [16] Rosenquist TH, Finnell RH, *Genes, folate and homocysteine in embryonic development*, Proc Nutr Soc, 2001, 60(1):53–61.
- [17] Chen PS, Wang CC, Bortner CD, Peng GS, Wu X, Pang H, Lu RB, Gean PW, Chuang DM, Hong JS, *Valproic acid and other histone deacetylase inhibitors induce microglial apoptosis and attenuate lipopolysaccharide-induced dopaminergic neurotoxicity*, Neuroscience, 2007, 149(1):203–212.
- [18] Huang Y, Tang X, Xie W, Zhou Y, Li D, Yao C, Zhou Y, Zhu J, Lai L, Ouyang H, Pang D, *Histone deacetylase inhibitor significantly improved the cloning efficiency of porcine somatic cell nuclear transfer embryos*, Cell Reprogram, 2011, 13(6): 513–520.
- [19] Phiel CJ, Zhang F, Huang EY, Guenther MG, Lazar MA, Klein PS, *Histone deacetylase is a direct target of valproic acid, a potent anticonvulsant, mood stabilizer, and teratogen*, J Biol Chem, 2001, 276(39):36734–36741.
- [20] Murko C, Lagger S, Steiner M, Seiser C, Schoefer C, Pusch O, *Histone deacetylase inhibitor Trichostatin A induces neural tube defects and promotes neural crest specification in the chicken neural tube*, Differentiation, 2013, 85(1–2):55–66.
- [21] Rijnboutt S, Jansen G, Posthuma G, Hynes JB, Schomagel JH, Strous G, *Endocytosis of GPI-linked membrane folate receptor-alpha*, J Cell Biol, 1996, 132(1–2):35–47.
- [22] Stanisławska-Sachadyn A, Mitchell LE, Woodside JV, Buckley PT, Kealey C, Young IS, Scott JM, Murray L, Boreham CA, McNulty H, Strain JJ, Whitehead AS, *The reduced folate carrier (SLC19A1) c.80G>A polymorphism is associated with red cell folate concentrations among women*, Ann Hum Genet, 2009, 73(Pt 5):484–491.
- [23] Zhao R, Goldman ID, *Folate and thiamine transporters mediated by facilitative carriers (SLC19A1-3 and SLC46A1) and folate receptors*, Mol Aspects Med, 2013, 34(2–3):373–385.
- [24] Clapés S, Fernández T, Suárez G, *Oxidative stress and birth defects in infants of women with pregestational diabetes*, MEDICC Rev, 2013, 15(1):37–40.
- [25] Maeng YS, Choi HJ, Kwon JY, Park YW, Choi KS, Min JK, Kim YH, Suh PG, Kang KS, Won MH, Kim YM, Kwon YG, *Endothelial progenitor cell homing: prominent role of the IGF2-IGF2R-PLCβ2 axis*, Blood, 2009, 113(1):233–243.
- [26] Blazer LL, Roman DL, Chung A, Larsen MJ, Greedy BM, Husbands SM, Neubig RR, *Reversible, allosteric small-molecule inhibitors of regulator of G protein signaling proteins*, Mol Pharmacol, 2010, 78(3):524–533.
- [27] Kach J, Sethakorn N, Dulin NO, *A finer tuning of G-protein signaling through regulated control of RGS proteins*, Am J Physiol Heart Circ Physiol, 2012, 303(1):H19–H35.
- [28] Druckenbrod NR, Powers PA, Bartley CR, Walker JW, Epstein ML, *Targeting of endothelin receptor-B to the neural crest*, Genesis, 2008, 46(8):396–400.
- [29] Matsumoto N, Kubo A, Liu H, Akita K, Laub F, Ramirez F, Keller G, Friedman SL, *Developmental regulation of yolk sac hematopoiesis by Kruppel-like factor 6*, Blood, 2006, 107(4): 1357–1365.
- [30] McConnell BB, Yang VW, *Mammalian Krüppel-like factors in health and diseases*, Physiol Rev, 2010, 90(4):1337–1381.
- [31] Ruddy DA, Kronmal GS, Lee VK, Mintier GA, Quintana L, Domingo R Jr, Meyer NC, Irlin A, McClelland EE, Fullan A, Mapa FA, Moore T, Thomas W, Loeb DB, Harmon C, Tsuchihashi Z, Wolff RK, Schatzman RC, Feder JN, *A 1.1-Mb transcript map of the hereditary hemochromatosis locus*, Genome Res, 1997, 7(5):441–456.
- [32] Kim Y, Paroush Z, Nair K, Hafen E, Jiménez G, Shvartsman SY, *Substrate-dependent control of MAPK phosphorylation in vivo*, Mol Syst Biol, 2011, 7:467.
- [33] Caldwell RB, Kierzek AM, Arakawa H, Bezzubov Y, Zaim J, Fiedler P, Kutter S, Blagodatski A, Kostovska D, Koter M, Plachy J, Carninci P, Hayashizaki Y, Buerstedt JM, *Full-length cDNAs from chicken bursal lymphocytes to facilitate gene function analysis*, Genome Biol, 2005, 6(1):R6.
- [34] Hui KK, Kanungo AK, Elia AJ, Henderson JT, *Caspase-3 deficiency reveals a physiologic role for Smac/DIABLO in regulating programmed cell death*, Cell Death Differ, 2011, 18(11):1780–1790.

- [35] Burk RF, Hill KE, *Selenoprotein P-expression, functions, and roles in mammals*, *Biochim Biophys Acta*, 2009, 1790(11): 1441–1447.
- [36] Malcherek G, Mayr L, Roda-Navarro P, Rhodes D, Miller N, Trowsdale J, *The B7 homolog butyrophilin BTN2A1 is a novel ligand for DC-SIGN*, *J Immunol*, 2007, 179(6):3804–3811.

Corresponding author

Chiung-Chi Peng, Graduate Institute of Clinical Medicine, College of Medicine, Taipei Medical University, 250 Wu-Shing Street, 11031 Taipei, Taiwan; Phone +886–2–27361661, Fax +886–2–27294931, e-mail: misspeng@ms2.hinet.net

Received: June 23, 2013

Accepted: December 13, 2013